Non-destructive evaluation of the mechanical behaviour of chestnut wood in tension and compression parallel to grain

Artur O. Feio[1], *Paulo B. Lourenço*[2, *] *& José S. Machado*[3]

[1] PhD Student, Department of Civil Engineering, University of Minho, Azurém, P-4800-058 Guimarães, Portugal. Phone: +351 253 510 200, fax: +351 253 510 217, email: af@civil.uminho.pt

[2, *] Corresponding author. Associate Professor, Department of Civil Engineering, University of Minho, Azurém, P-4800-058 Guimarães, Portugal. Phone: +351 253 510 209, fax: +351 253 510 217, email: pbl@civil.uminho.pt

[3] Research Officer, National Laboratory for Civil Engineering, Timber Structures Division, Lisbon, Portugal. Phone: +351 21 8443299, fax: +351 21 8443025, email: saporiti@lnec.pt

Abstract: The paper addresses the evaluation of strength and stiffness of chestnut wood, in tension and compression parallel to the grain, using different non-destructive techniques (ultrasounds, Resistograph and Pilodyn). Around two hundred timber specimens (divided into compression and tension tests) were tested up to failure, comprising recently sawn timber (which is now available on the market for structural purposes) and what was called old wood, obtained from structural elements belonging to ancient buildings. The possibility of predicting wood properties by application of non-destructive techniques is discussed based on simple linear regression models. Extrapolation of regression models obtained from recent cut wooden material to that obtained from old timber beams is analysed. The results show reasonable correlations between mechanical elastic properties and non-destructive techniques (ultrasounds, Resistograph and Pilodyn). New and old wood mechanical data exhibited a scattered cloud of points, implying in terms of assessment of properties of timber elements in service by regression models that these models should not be supported only on data from recently sawn wood. Therefore, models combining information from new and old wood specimens are proposed based on lower 95% confidence limits of regression lines.

Keywords: chestnut wood, compression parallel to the grain, non-destructive evaluation, Pilodyn, Resistograph, tension parallel to the grain, ultrasounds.

1. Introduction

Timber structures survey is the first and crucial step for deciding on timber structural elements capability for assuring the desired performance over an expected service life. The scope of survey includes the necessity of gathering information on wood species, expected service class and deterioration, besides other aspects such as geometrical survey, historical data gathering and technological traces that are of relevance for any historical structure, see e.g. (ICOMOS, 2001) for recommendations and methodology. Wood species identification is essential for defining a range of mechanical, physical and durability properties. Only then, non-destructive techniques (including visual strength grading) should be used for assessing possible characteristic values to be allocated to the wood members.

Wooden structures may suffer deterioration with time due to different causes (biological, instability, deterioration of joints and deformation or accidental damage) but in the majority of cases the damage observed in historical timber structures deals with biodeterioration and mechanical deterioration induced both by excessive moisture content. If no damaging action occurred, the impact of loading history and time over strength and stiffness of structural timber elements seems to be limited. Studies show no evidence of time-in-service effect over old timber beams strength and stiffness parallel to grain, possibly due to being subjected during service to permanent low stress levels. Usually, inspection of old timber structures shows that large deformations are the result of using green round or square elements and excessive moisture conditions during the history of the structure.

In order to assess the safety of old structures and preserve the original fabric as much as possible, *in situ* inspection and evaluation of actual mechanical properties represent a first step towards diagnosis, structural analysis and the definition of possible

remedial measures (Ross et al. 1997; Bertolini et al. 1998). The inspection results, combined with historical information and a visual survey, can also be the support of maintenance decisions. Non-destructive evaluation (NDE) is already widely applied to the control of structural integrity, due its characteristics of reliability, simplicity and low cost. However in order to apply non-destructive techniques it is mandatory to possess a relation between non-destructive parameters and mechanical characteristics of wood (Kasal and Anthony 2004). Unfortunately there is no guarantee that such relation is unique for all wood species, as already observed in machine strength grading, and therefore extrapolations must be observed very carefully.

Timber structures design usually considers the exceptional capacity of wood to withstand loading parallel to the grain. Furthermore given the low strength of timber when loaded perpendicularly to the grain, a rule of thumb consists of avoiding tensile stresses perpendicular to the grain (Bonamini et al. 2001; Zwerger 2000). The most relevant material properties along the grain are compression and tension. Compressive strength parallel to the grain of clear wood is between 40 and 60 percent of the bending strength in that direction and between 30 and 50 percent of the tensile strength (USDA 1999).

The modulus of elasticity for wood parallel to grain exhibits moderate dependency of the type of loading: tension, compression or even bending. However European standards adopt for timber a modulus of elasticity parallel to grain obtained from a bending test. Gehri (1997) reported a modulus of elasticity in compression ($E_{c,0}$) lower than the corresponding modulus of elasticity in bending ($E_{m,0}$), which in turn is lower than the corresponding modulus of elasticity in tension ($E_{t,0}$):

$$E_{c,0} \leq E_{m,0} \leq E_{t,0} \qquad (1)$$

Although generally mechanical properties of structural timber members are driven by defects, clear wood properties are relevant when dealing with strength and stiffness of upper strength grades (visual or mechanical). Also in critical points in timber structures (joints or high stressed zones) the good practice leads generally to avoid the presence of features that can have a reducing effect on strength or stiffness, meaning that ultimate capacity of timber structures will be significantly determined by clear wood properties (density, strength and stiffness). Moreover, regular non-destructive strength grading methods (visual and mechanical) are often not applicable to the appraisal of a single beam in-service, being therefore possible to allocate strength values to particular timber element by applying reduction factors (due to strength-reducing features) to clear wood properties.

The objective of this paper is to discuss the possibility of using NDE methods for the evaluation of strength and stiffness of chestnut clear wood (*Castanea sativa* Mill.) in compression and tension parallel to grain. Regression models using data from recently sawn and from old timber beams were used in order to discuss the possibility of extrapolating models obtained from recently sawn timber to the appraisal of mechanical properties of timber elements in service. For this purpose, the paper presents several correlations between mechanical properties, density and non-destructive methods (ultrasounds, Resistograph and Pilodyn).

2. Description of test specimens

Chestnut wood (*Castanea sativa* Mill.) is usually present in historical Portuguese buildings. For the present testing program, two groups of chestnut clear wood specimens were selected. One designated as *New Chestnut Wood* (NCW) - recently sawn timber - was obtained from wood material produced in the North of Portugal. The

other group designated as *Old Chestnut Wood (OCW)* was obtained from timber beams from the demolition of ancient buildings located in the North of Portugal. The specialist contractor providing the "old" wood claims that the age of the timber logs is in the range of 50 to 200 years, and the load-history while in service is unknown. Dendrochronological data (annual ring density profile and pattern) was not obtained from old wood beams.

Wood specimens from old beams were included having in mind possible changes of wood quality used in construction (due to changes in forest management or quality criteria followed when selecting timber elements), enlarging in this way the spectrum of chestnut wood properties tested. Therefore a possibility of discussing the soundness of applying regression models obtained from recently sawn timber to old timber beam is foreseen.

In order to ensure comparable and reliable results, before testing, all specimens were conditioned in a climatic room capable of keeping constant temperature (20 ± 2ºC) and humidity (65 ± 5%) until constant mass was reached.

2.1 Compressive tests

In total, 94 specimens with dimensions 50×50×300 mm were adopted for ultrasonic testing. Afterwards, the specimens were cut in two smaller specimens, with dimensions of 50×50×100 mm and 50×50×200 mm: the first specimen was used for the additional non-destructive tests (Resistograph and Pilodyn 6J) and the second specimen was tested in laboratory up to failure, see Figure 1a. The latter specimens have the dimensions recommended by ASTM standard D143 (1994).

2.2 Tensile tests

In total, 84 specimens were selected after visual inspection ensured that the gauge length was kept clear of defects. To prevent fracture at the grips care was taken avoiding

knots at the transition from test length to the clamped section. According to the standard Nbr7190 (1997), the specimens adopted must possess a geometry as the one represented in Figure 1b. Their overall length was 330mm while the "gauge length" was 210mm long and about 7mm in thickness. Tension grips length available only seized half of the specimen grip length, which led to failure in the close vicinity of the bottleneck region of the specimens, during preliminary tests. Tensile specimens were then modified (see again Figure 1b), taking into account the effective grip area of the testing equipment. Additional trial tests showed that this change assured occurrence of tension failure modes in the middle third of the specimen. Ultrasonic tests were also carried out in these specimens before testing them up to failure.

3. Characterization of physical and mechanical properties

3.1 Density

Given the conditioning of the specimens, the average density ρ_m is determined for a moisture content of 12%, obtained by the ratio between mass *m* and volume *V*:

$$\rho_{12\%} = \frac{m_{12\%}}{V_{12\%}} \qquad (2)$$

Table 1 presents the average density and coefficient of variation according to the type of loading and type (age) of wood specimens. On average and for the complete 178 specimens sample, the densities of NCW (627.3 kg/m^3) and OCW (589.2 kg/m^3) groups are similar, showing NCW only in average a density 6% higher than OCW. High coefficients of variation found for tension specimens (10%) as regards compression (3%) are probably caused by lower accuracy on volume determination due to specimens' geometry.

3.2 Compressive tests

Mechanical testing was carried out using a Baldwin universal testing machine, with a load cell of 300 kN. A power supply Schenk equipment was used, together with a HBM system (Spider 8) for the acquisition and amplification of the data, see Figure 2a. Lateral deformation was assessed by using strain gauges attached to all faces of the specimens (DD1 type from HBM, with a range of ± 2.5 mm, a sensitivity of ± 2.5 mV/V and a linear deviation of ± 0.05%). Vertical deformation (crosshead to platen) was measured using two LVDT (range ± 2.5 mm).

The adopted test procedure follows the Brazilian Standard NBr 7190 (1997), which includes two preliminary loading-unloading cycles before continuously increasing loading up to failure. A loading rate of 6×10^{-3} mm/s, in the preliminary loading-unloading phase, and of 4×10^{-2} mm/s in the failure phase was applied, being the stress-strain diagrams continuously recorded. The compressive strength $f_{c,0}$ parallel to the grain was determined by the maximum load applied to the specimen, and the modulus of elasticity parallel to grain $E_{c,0}$, given by the secant modulus defined as the slope of the linear part in the stress-strain curve, was obtained by

$$E_{c,0} = \frac{\sigma_{50\%} - \sigma_{10\%}}{\varepsilon_{50\%} - \varepsilon_{10\%}} \qquad (3)$$

where $\sigma_{10\%}$ and $\sigma_{50\%}$ are the stresses corresponding to 10% and 50% of the failure conventional stress, and $\varepsilon_{10\%}$ and $\varepsilon_{50\%}$ are the strains corresponding to the values of $\sigma_{10\%}$ and $\sigma_{50\%}$. The stress is obtained as the load cell value divided by the cross section area of the specimen and the strain is obtained as the average of the displacements measured in the (two) vertical LVDTs. Finally, the Poisson ratios were calculated equally as secant values for the same stress range of the conventional failure stress.

The time elapsed between the tests and withdrawal of the specimens from the climatic chamber (less than 24 hours) did not affect the conditioning of the specimens. The results of the uniaxial compression tests are presented in Table 2. The values for the coefficient of variation CV are relatively large (average CV of 15% for the strength values and values ranging between 8 and 16% for the elasticity modulus) but well within the variability found for wood species tested in compression parallel to the grain. Results obtained for OCW and NCW groups are similar. These results support decisions often made to allocate strength and stiffness values at timber elements in service using data obtained from recently sawn timber from the same wood species (Kuipers 1986). Nevertheless, it is interesting to observe that, in this particular sample, the compressive strength of old chestnut wood $f_{c,0}$ is 11% higher than new chestnut wood. This is in opposition with the density values, where the density of OCW is 10% lower than NCW (Table 1). The results indicate thus that a simple correlation of density and strength is not possible when old and new wood are being compared.

Figure 2b illustrates typical failure patterns observed in compression parallel to the grain. During experiments gross localization band(s) were easily identified running approximately perpendicular to the longitudinal axis on the radial plane and obliquely, at an angle between 45º and 70º relative to the longitudinal axis, on the tangential plane. Kink formation origins considerable loss of stiffness and after peak load a localization gross band appears, see Figure 2c. It was also observed that each specimen develops one or, at maximum, two principal gross localization band(s) observable with the naked eye. This/these band(s) occur at relatively large strains (1.6-2.1%), i.e. at a strain beyond the maximum stress ($f_{c,0,\max}$) and reach widths between 0.2 mm and 1.1 mm. This localization band is followed by a considerable increase in lateral deformation.

3.3 Tensile tests

Mechanical testing was carried out using a universal testing machine (INSTRON – Model 4483), with a load cell of 100 kN. Additionally a feed, acquisition and amplification data system was defined for testing, which allows to obtain and register all data, see Figure 3.

The measurements of the vertical and horizontal strains in the specimens were done by two pairs of bonded strain gauges, placed on opposite faces of the specimens to eliminate the effect of bending due to load eccentricities. The pair of vertical strain gauges (parallel to the grain) and the pair of horizontal strain gauges (perpendicular to the grain) were mounted in the central section of the specimens. This measured strain is considered to represent strain at a point acceptable from a macro-mechanics perspective, considering that wood is an inhomogeneous material at a microscopic scale.

All strain gauges were wired in a full bridge configuration with one dummy gauge as temperature compensation strain gauge. Before gluing the strain gauges, wood specimens were slightly polished with abrasive paper and wiped with acetone.

The adopted test procedure follows the Brazilian Standard NBr 7190 (1997), which includes two loading-unloading cycles before continuously increasing loading up to failure. The loading rate was fixed at 5×10^{-2} mm/s for the entire test. Each load-extension curve was reduced to a true stress-true strain plot; from these, the tensile strength parallel to grain $f_{t,0}$ is defined as the conventional value determined by the maximum strength applied to a specimen or as the conventional value corresponding to a strain equal to a 0.3% offset in the usual terminology, whichever is lower.

The stiffness of wood, in tension parallel to the grain, is determined by its modulus of elasticity $E_{t,0}$, defined as above. Finally, the Poisson ratios were calculated equally as secant values for the same stress range of the conventional failure stress.

The tests results are presented in Table 2. Once again, the coefficients of variation are relatively large (ranging between 19 and 29%) but within the variability found for wood species and the presence of small material defects (namely local grain deviations). The difference in the results between old and new wood is very low, which seems in agreement with the values of density found for the sample, see Table 1. The results also indicate a marginal (5%) difference between average compressive and tensile strength but a significant difference in modulus of elasticity ($E_{c,0} = 0.66\ E_{t,0}$).

Generally, failure in tension parallel to the grain follows one of the patterns shown in Figure 4a-d, namely shear, a combination of shear and tension, pure tension and splinter mode.

4. Description of non-destructive test procedures

4.1. Resistograph tests

The Resistograph is a commercial testing equipment based on micro-drilling wood at constant speed, and on measuring the energy required for maintaining such speed. It is usually adopted to obtain density profiles of wood. In the present testing program, drilling was made parallel to plane RT (planes TL and LR), which, in real cases, represents the accessible faces of timber elements. Here, R stand for radial, T stands for tangential and L for longitudinal, see also Figure 1. Plane RT is defined by the radial and tangential axes, meaning that it is a plane perpendicular to the longitudinal axis of the element, coinciding with the longitudinal axis of wood. For each specimen, three independent profiles have been carried out and the results shown represent the average of the readings. The adopted equipment was provided by Rinntech, including a 12 bit precision, a 1/100 mm resolution, a drill with a diameter of 3 mm (drill tip) and 1.5 mm (drill shaft), and a drilling length of 450 mm.

For all wood specimens, a resistographic measure (*RM*) was calculated from the drilling profile curve obtained with the Resistograph, as the ratio between the area of the profile diagram and the length *l* of the drilled perforation (see Eq. 4). Using this scalar, the Resistograph results can be easily compared with the values of density and of the elastic properties. Scalar RM could be divided by the size of the drill tip, in order to remove the influence of the drill diameter but this would be misleading and the results provided by the equipment cannot be directly correlated with the drill diameter. The Resistograph was only used in compression specimens.

$$RM = \frac{Area\,of\ \ profile}{l} \tag{4}$$

4.2. Pilodyn 6J tests

The Pilodyn 6J is a device that, through the release of a spring, transforms the elastic potential energy of a metallic needle with 2.5 mm of diameter into impact energy (penetration depth). The penetration depth (related to surface hardness or to resistance to superficial penetration) is regarded as inversely proportional to wood density. Measurement was performed on planes TL and LR. For each specimen, three independent impact tests were carried out and the results (correlation with density and mechanical and elastic properties) presented are the average of the readings made. The Pilodyn test was only applied to compression specimens.

4.3. Ultrasonic tests

The ultrasonic tests were carried out using the equipment Pundit/Plus, with cylinder-shaped transducers of 150 kHz. In all tests, coupling between the transducers and specimens was assured by a conventional hair gel, and a constant pressure was applied by means of a rubber spring, allowing adequate transmission of the elastic wave between the transducers and the specimen under testing.

The propagation velocity of the longitudinal stress waves in elastic media depends essentially on the stiffness and the density of the media. For prismatic, homogeneous and isotropic elements and for those with a section width smaller than the stress wavelength, the relation:

$$E_{din} = u^2 \cdot \rho \qquad (5)$$

holds, where E_{din} represents the dynamic modulus of elasticity (N/mm²); u is the propagation velocity of the longitudinal stress waves (m/s), usually denoted by UPV (ultrasonic pulse velocity) and ρ is the density of the specimens (kg/m³).

4.3.1. Compression specimens

For the compressive specimens, two methods were used for ultrasonic measurements in the framework of a more general approach, see Figure 5a (Indirect Method – IM – and Direct Method – DM – parallel to the grain). Nevertheless, the only method reported in this paper is the IM, since it is the most appropriate in practical cases. The IM can be used for evaluating different zones of the element (global or local evaluation) and only needs a face of the element to be accessible. Regarding the DM, it requires access to the ends of the elements (in most cases not possible) and allows only a global evaluation of the material (it is not possible to evaluate weak or critical zones).

For each specimen, three independent ultrasonic tests have been carried out and the results shown represent the average of the readings. OCW group present higher UPV values (+12%) when compared with the NCW group, Table 3. This result is in accordance with the strength and stiffness values obtained, Table 2, but not in agreement with the density values given in Table 1. Using Eq. (5) and assuming E_{din}

proportional to E, the ratio $(E/\rho)_{new}$ reads 11.9×10^9 mm^2/s^2 and $(E/\rho)_{old}$ reads 15.1×10^6 mm^2/s^2, confirming that the $UPV_{old} \approx (15.1/11.9)^{0.5} = 1.13\ UPV_{new}$.

4.3.2. Tensile specimens

For the tensile specimens, three different types of tests were carried out: (a) Indirect Method (d = 20 cm); (b) Indirect Method (d = 45 cm) and (c) Direct Method, parallel to the grain (see Figure 5b). The propagation times of the ultrasonic wave were recorded and the material was assumed to be continuous and homogeneous. Again, for each specimen, three independent ultrasonic tests have been carried out and the results shown represent the average of the readings. The only method reported here is the IM, since it is the most appropriate in practice. IM ultrasonic testing induces a complex wave interaction (modes of propagation) that results on a considerable effect of propagation length on UPV. Since the larger measuring base for the indirect method provides more comparable values to the ones obtained by the direct method only results covering that larger measuring base (d = 45cm, Figure 5) are presented in this paper.

Table 3 shows again the differences between the two considered groups in terms of wood age. The main conclusion is again that the OCW group presents slightly higher values (+5.8%) when compared with the NCW group. The difference found between OCW and NCW is not corroborated by the density and elasticity modulus values found for this sample, which are almost equal, see Table 1 and Table 2.

5. Linear correlations based on the NDT methods

The previous sections addressed destructive testing and non-destructive techniques under very well defined conditions, using small clear wood specimens. The reader must be aware that in the application of the linear correlations presented in this section to historical structures only the sound part of the wood can be tested and graded.

Moreover, the actual *in situ* measurements can be made in conditions substantially different from the ones adopted here.

5.1. Compression tests

5.1.1. Correlations with density

Figure 6 shows the correlations between the RM and the density for NCW and OCW. Moderate correlations are found between the two quantities when the results are analysed separately. However, when the results are analysed together, good correlations are obtained. For practical purposes, it is recommended to use this measure carefully as a quantitative indicator. For practical applications, in order to assure a conservative approach, a lower 95% confidence limit equation considering all results is proposed:

$$\rho = 224.29 + 1.06 \cdot RM \quad [\text{kg/m}^3], \text{ with RM in [bits]} \qquad (6)$$

Figure 7 shows the correlations between the needle penetration and the density for NCW and OCW. The scatter in the results is low and a good correlation between the two quantities is found. Once again, when the results are analysed together the correlations improve. The lower 95% confidence limit equation, considering all results, is given by:

$$\rho = 1001.99 - 51.81 \cdot Penetration \, [\text{kg/m}^3], \text{ with } Pen \text{ in [mm]} \qquad (7)$$

It is noted that the needle penetrates only 6.5 to 10 mm, or between one and three annual growth rings. Therefore, the result is superficial and care is needed in practical applications, verifying if the outer surface is deteriorated due to biological attack.

5.1.2. Correlations with the elasticity modulus

Figure 8 shows the correlations between the UPV and $E_{c,0}$ using the IM. Only moderate linear correlations are found with a very large difference between NCW and OCW.

Also, these results are in agreement with Table 3 and the discussion provided in the previous section. Considering all tests, a lower 95% confidence limit is given by:

$$E_{c,0} = -3384.86 + 1.82 \cdot UPV \ \text{[N/mm}^2\text{]}, \text{ with } UPV \text{ in [m/s]} \quad (8)$$

Figure 9 shows the correlations between the RM and the elasticity modulus for NCW and OCW. Moderate linear correlations were found. For practical purposes, it is not recommended to use this measure as a quantitative indicator. Considering all tests together, no significant correlation is obtained. Figure 10 shows the correlations between the penetration reached with the needle of the Pilodyn device and the elasticity modulus for NCW and OCW, which were found to be moderate. Once again, the global results present no significant correlation.

5.1.3. Correlations with the uniaxial compressive strength

Figure 11 shows the weak linear correlations between the UPV and $f_{c,0}$ using the IM. Considering all tests together, a lower 95% confidence limit is given by:

$$f_{c,0} = -17.95 + 8.22 \times 10^{-3} \cdot UPV \ \text{[N/mm}^2\text{]}, \text{ with } UPV \text{ in [m/s]} \quad (9)$$

Figure 12 shows the correlations between the RM and the uniaxial compressive strength for NCW and OCW. Moderate linear correlations were found. For practical purposes, it is not recommended to use this measure as a quantitative indicator. Considering all tests together, no significant relations were obtained. Figure 13 shows that the correlation between the penetration reached with the needle of the Pilodyn device and the uniaxial compressive strength for NCW and OCW were found to be not significant. Once again, the global results present no significant correlation.

5.2. Tension tests

5.2.1. Correlations with the elasticity modulus

Figure 14 shows the correlations found between UPV and $E_{t,0}$ using ultrasonic testing according to the IM. Moderate correlations were found for the OCW and NCW groups being visually possible to identify a distinct cloud points shape for each group. Therefore each group shows a lower variability than the sample joining the two groups.

In order to cope with this variability and to assure an acceptable level of safety when predicting clear wood modulus of elasticity in tension, it is proposed the adoption of confidence intervals. Therefore a predictive equation based on the lower 95% confidence limit is given by:

$$E_{t,0} = -19087.76 + 3.86 \cdot UPV \quad [\text{N/mm}^2], \text{ with } UPV \text{ in [m/s]} \qquad (10)$$

5.2.2. Correlations with the uniaxial tensile strength

The correlation between UPV and $f_{t,0}$ using IM method, is weak for the two groups, see Figure 15. As for the modulus of elasticity a predictive equation should combine OCW and NCW data and a lower 95% confidence limit equation is given by

$$f_{t,0} = -20.81 + 5.66 \times 10^{-3} \cdot UPV \quad [\text{N/mm}^2], \text{ with } UPV \text{ in [m/s]} \qquad (11)$$

6. Conclusions

The paper aims at characterizing density and mechanical properties along the grain of two groups of chestnut wood, differentiated as new and old according to the time in service, using NDT.

The two groups comprise clear wood specimens (reducing variability due to defects and allowing a better comparison of differences between samples) from the

same provenance (North of Portugal). Both groups show, in average, slightly higher tensile than compressive strength (≈6%) and a much higher modulus of elasticity in tension than compression (≈53%), see Table 4. Strength, stiffness and density values from both groups do not differ by more than 15%. The results contribute to the statement that sound old wood generally does not have worse mechanical characteristics than contemporary marketed wood of the same kind.

Single-parameter linear regressions are proposed for density, reasonable determination coefficients were established using RM (Resistograph) and needle penetration (Pilodyn) as independent variables, being this last NDT the best predictor of density (r^2 = 0.91). Regarding compression and tension strength moderate coefficients of determination were obtained using RM and UPV (ultrasounds) for compression (around 0.60 and 0.57, respectively) and UPV for tensile strength (r^2 = 0.32). For the modulus of elasticity, UPV gave coefficients of determination of 0.64 and 0.65 for compression and tension, respectively.

The results show also that the usage in practice of regression models might lead only to approximate conclusions when applied to old timber elements. Due to wood variability, the safe use of regression curves for predicting mechanical properties of chestnut timber elements in service imply models validation by removing samples from structural elements under inspection. Since this approach is not often reasonable or possible, lower 95% confident limit equations are given for predicting the mechanical capacity of chestnut clear wood properties along the grain using ultrasonic testing. However, due to the poor coefficients of determination obtained, this NDT technique can hardly be recommended for quantitative evaluation. For the Resistogragh and Pilodyn such approach is not possible at all due to the extreme disparity of a cloud point

scatter and, therefore, the use of these non-destructive methods for predicting mechanical properties along the grain is not recommended.

Acknowledgements

The financial support by the FCT under grant SFRH/BD/5002/2001 awarded to the first author is gratefully acknowledged.

References

1. American Society for Testing and Materials (1994). Standard methods of testing small clear specimens of timber. ASTM Designation: D143-94. ASTM, West Conshohocken, PA.
2. Bertolini, C., Brunetti, M., Cavallaro, P., Macchioni, N. (1998) A non destructive diagnostic method on ancient timber structures: some practical application examples. Proceedings of 5th World Conference on Timber Engineering. Montreux. Presses Polytechniques et Universitaires Romandes. Vol.I: pp. 456-465.
3. Bodig, J., Jayne, B. (1993) Mechanics of wood and wood composites. 2ªed: Krieger Publishing Company. ISBN 0-89464-777-6.
4. Bonamini, G., Noferi, M., Togni, M. and Uzielli, L. (2001). Handbook for Structural Timber: Vol. 1 – In situ Inspection and Diagnosis (in Italian). Mancosu Editore. Rome. ISBN-88-87017-01-8.
5. Brazilian standard (1997) Nbr7190 – Design of Timber Structures (in Portuguese). ABNT. Brazil.
6. Daniel, I., Ishai, O. (1994) Engineering mechanics of composite materials. Oxford University Press, New York, N.Y.

7. Gehri, E. (1997) Timber as a natural composite: explanation of some pecularities in the mechanical behaviour – Case: Assessment of the modulus of elasticity of timber parallel to grain. CIB-W18A/30-6-3.
8. Kasal, B., Anthony, R. (2004) Advances in in situ evaluation of timber structures. Prog. Struct. Engng. Mater. 6: pp. 94-103.
9. Kuipers, J. (1986) Effect of age and/or load on timber strength. Proceedings of 19th CIB-W18/19-6-1, Florence, Italy.
10. ICOMOS, Recommendations for the analysis, conservation and structural restoration of architectural heritage, 2001
11. Ross, R., DeGroot, R., Nelson, W., Lebow, P. (1997) The relationship between stress wave transmission characteristics and the compressive strength of biologically degraded wood. Forest Products Journal. 47(5): pp. 89-93 (1997).
12. USDA Wood Handbook (1999) Forest Service Agricultural Handbook, No. 72.
13. Zwerger K. (2000) Wood and wood joints: building traditions of Europe and Japan. Birkhäuser, Basel, Berlin, Boston. ISBN 3-7643-6333-9.

List of Figures

Figure 14 – Relation between the UPV and $E_{t,0}$ for the NCW and OCW groups.

Figure 15 – Relation between the UPV and $f_{t,0}$ for the NCW and OCW groups.

List of Tables

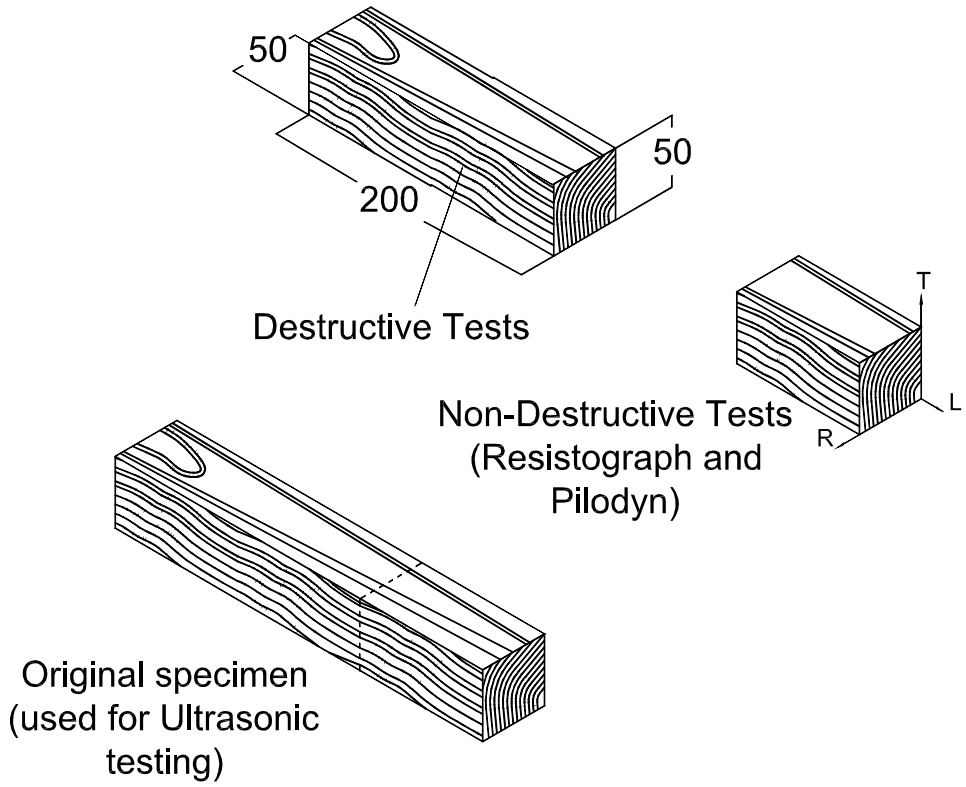

(a)

Figure 1 – Specimens used in the testing program (nominal dimensions in mm): (a) compressive and non-destructive tests, and (b) tensile tests.

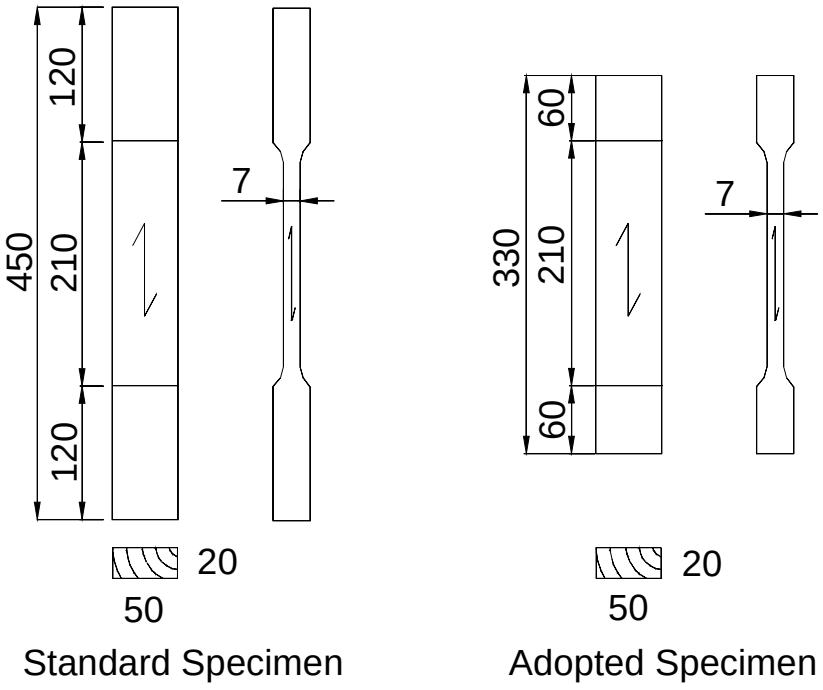

(b)

Figure 1 – Specimens used in the testing program (nominal dimensions in mm):

(a) compressive and non-destructive tests, and (b) tensile tests.

(a)

Figure 2 – Typical aspects of the compressive tests: (a) general view of the test set-up, (b) failure mode, and (c) stress-strain and lateral strain-longitudinal strain diagrams.

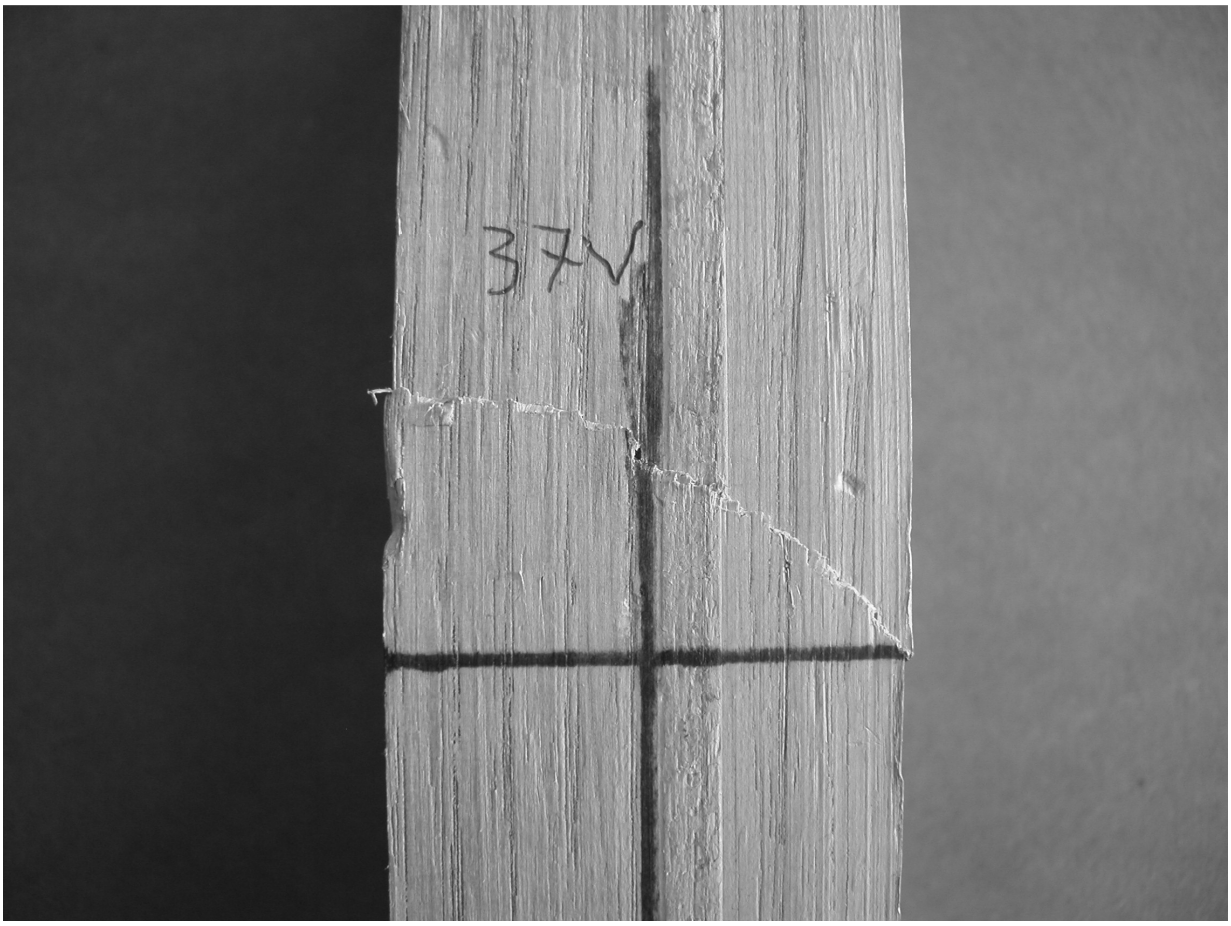

(b)

Figure 2 – Typical aspects of the compressive tests: (a) general view of the test set-up, (b) failure mode, and (c) stress-strain and lateral strain-longitudinal strain diagrams.

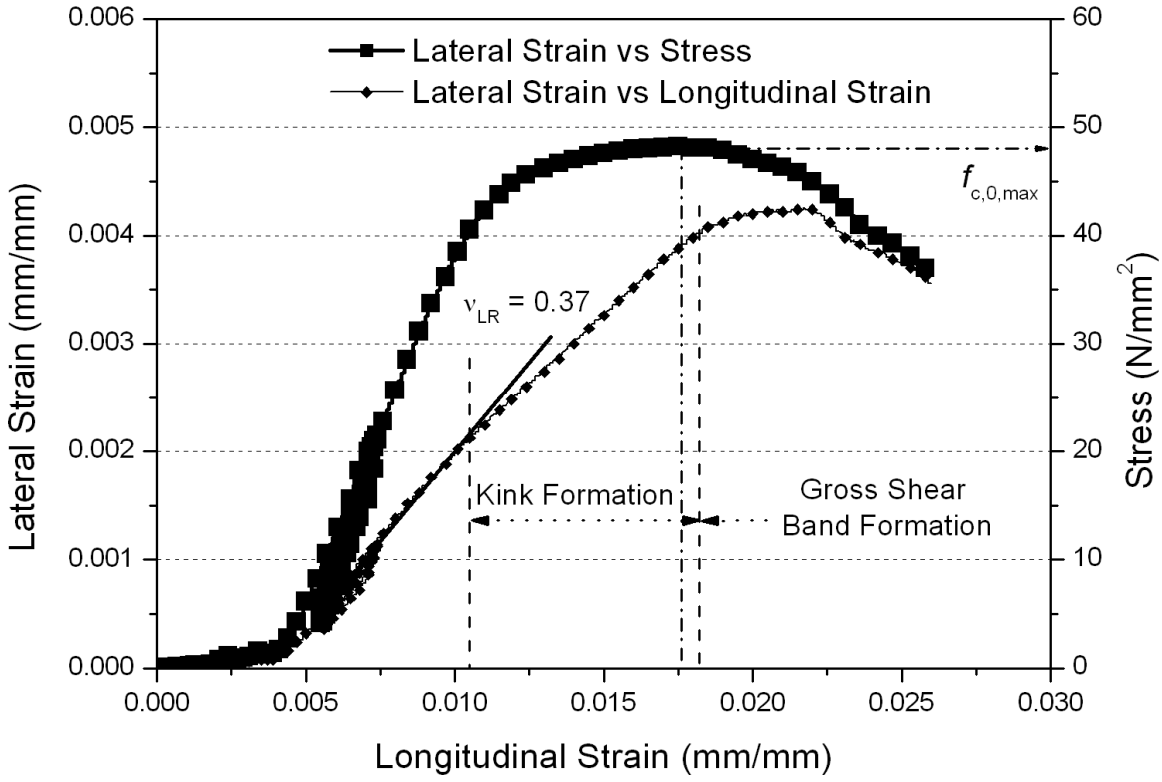

(c)

Figure 2 – Typical aspects of the compressive tests: (a) general view of the test set-up, (b) failure mode, and (c) stress-strain and lateral strain-longitudinal strain diagrams.

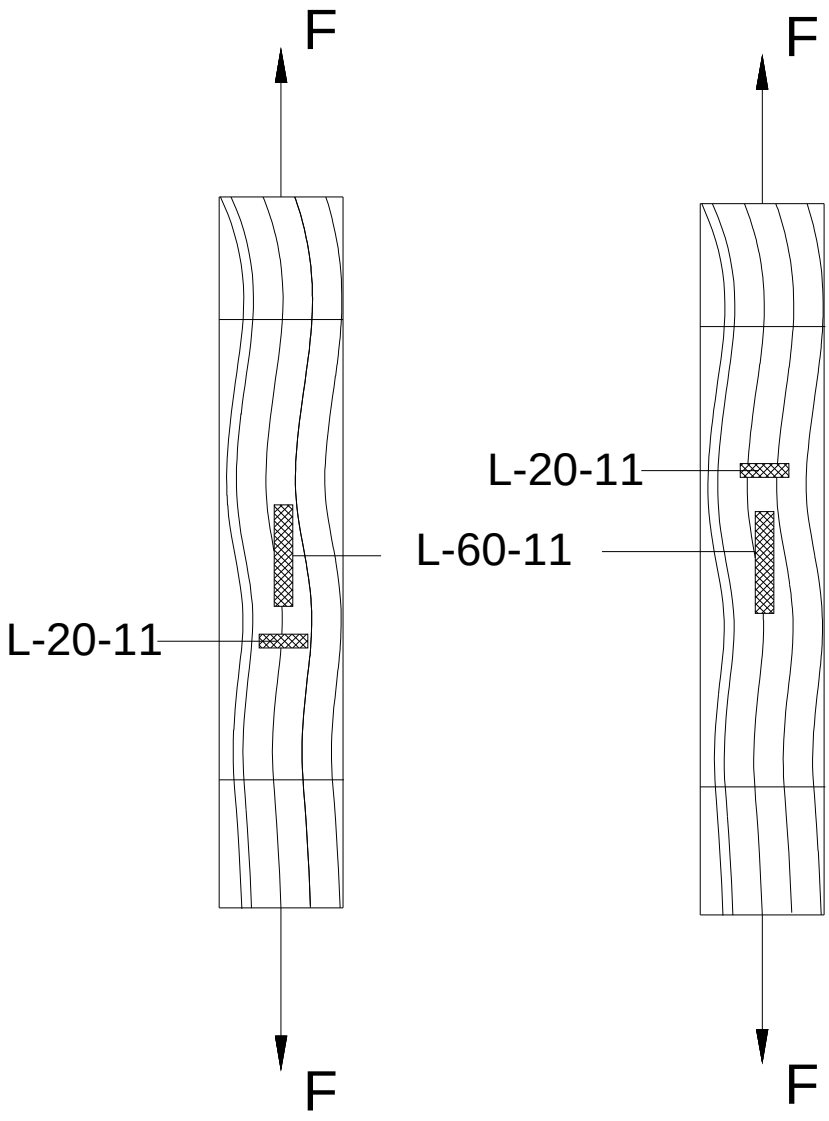

(a)

Figure 3 – Bonded strain gauges: (a) scheme in the two opposite faces; and (b) view of an instrumented specimen.

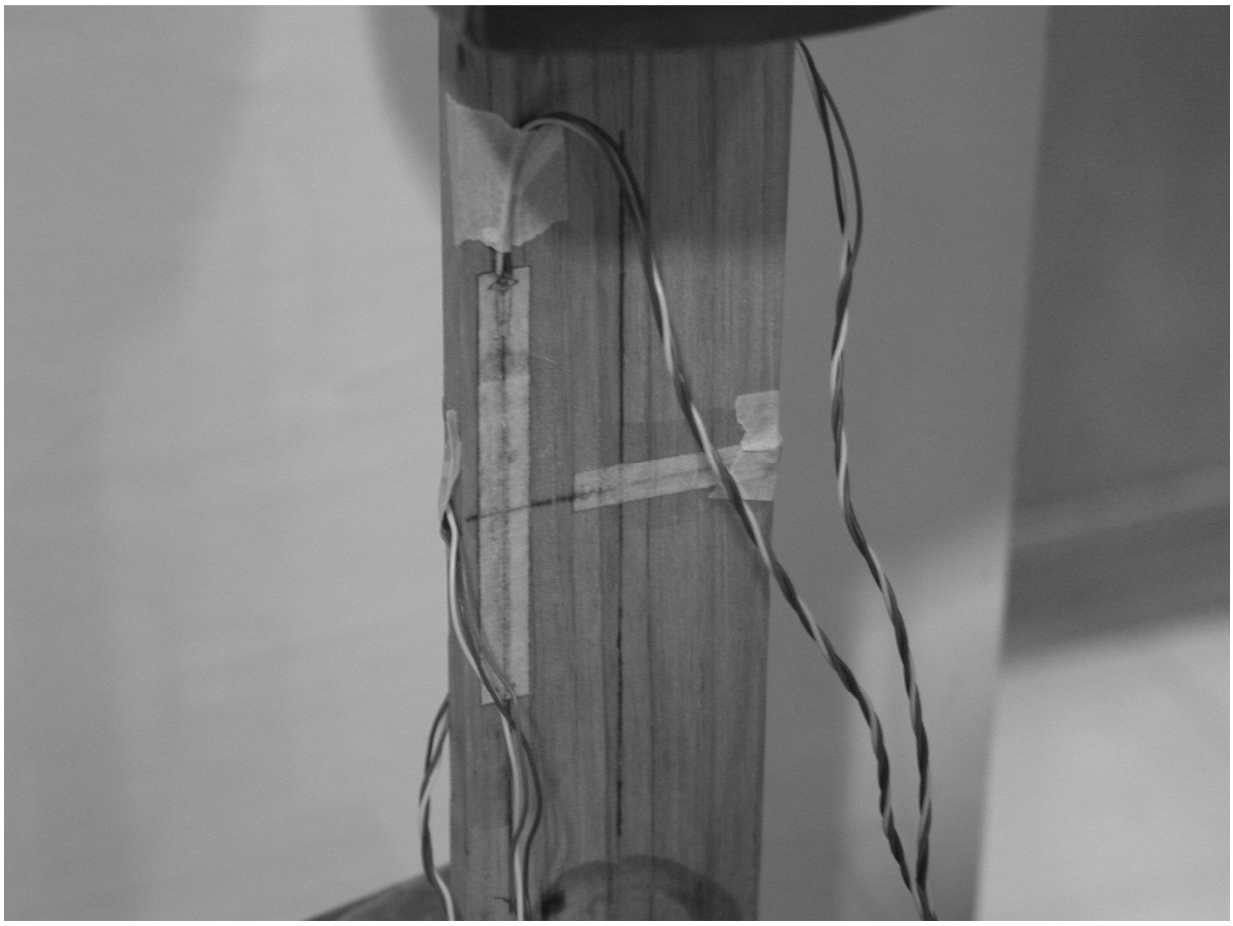

(b)

Figure 3 – Bonded strain gauges: (a) scheme in the two opposite faces; and (b) view of an instrumented specimen.

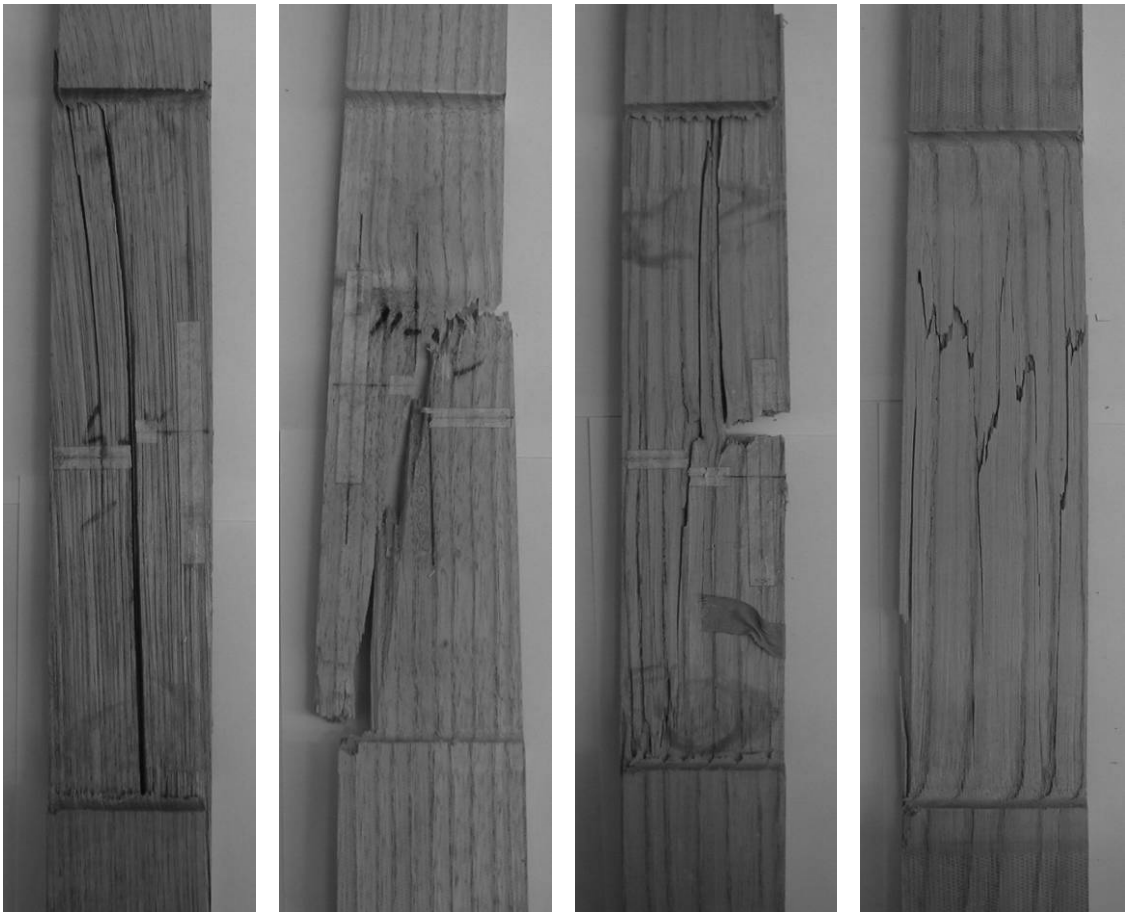

(a) (b) (c) (d)

Figure 4 – Typical aspects of the tensile tests: (a) shear, (b) shear and tension, (c) pure tension and (d) splinter failure modes

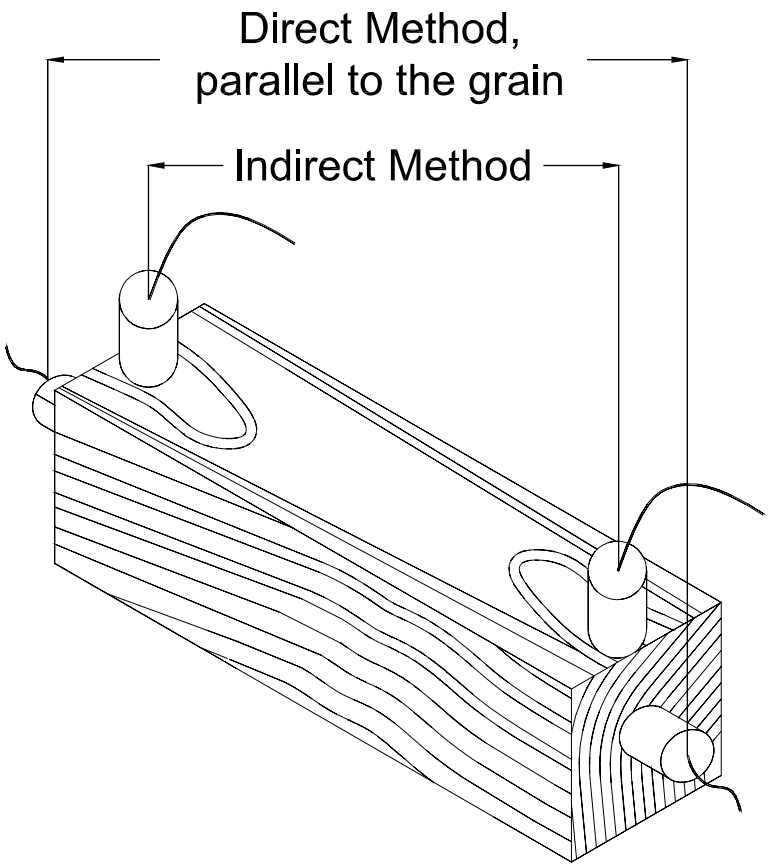

(a)

Figure 5 – Test set-up for ultrasonic testing: (a) compressive tests and (b) tensile tests.

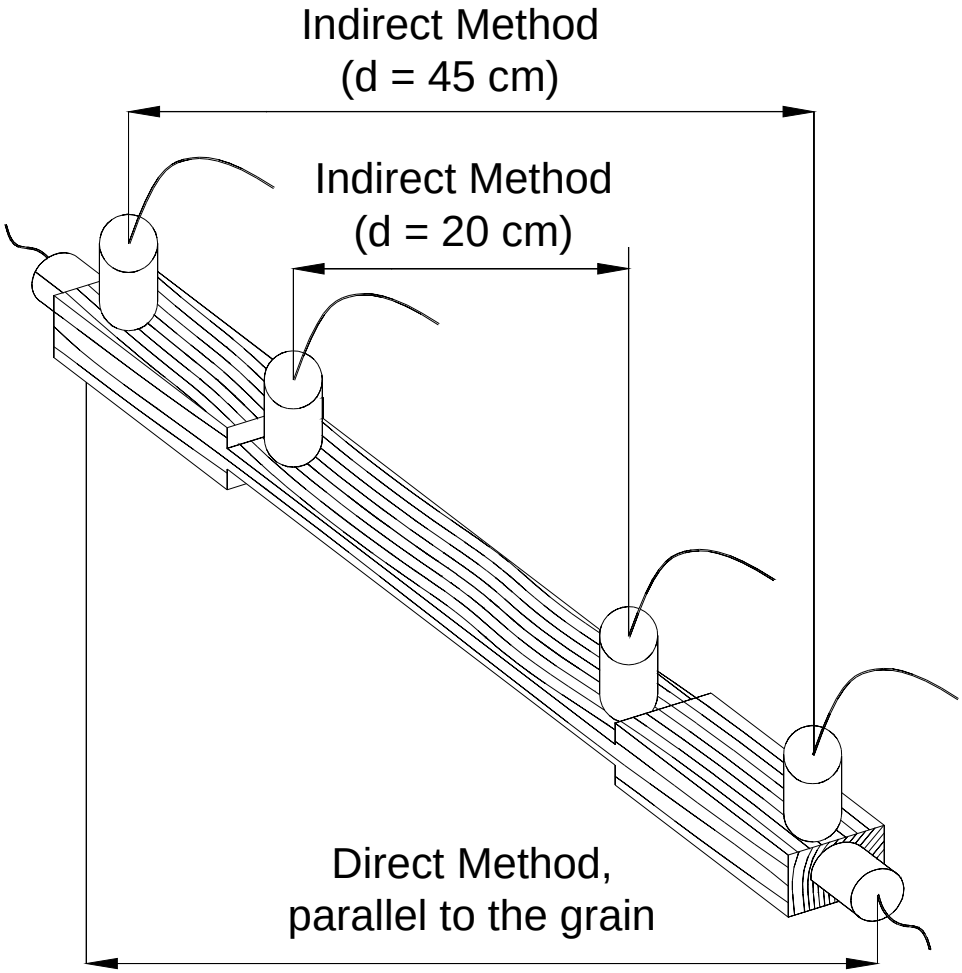

(b)

Figure 5 – Test set-up for ultrasonic testing: (a) compressive tests and (b) tensile tests.

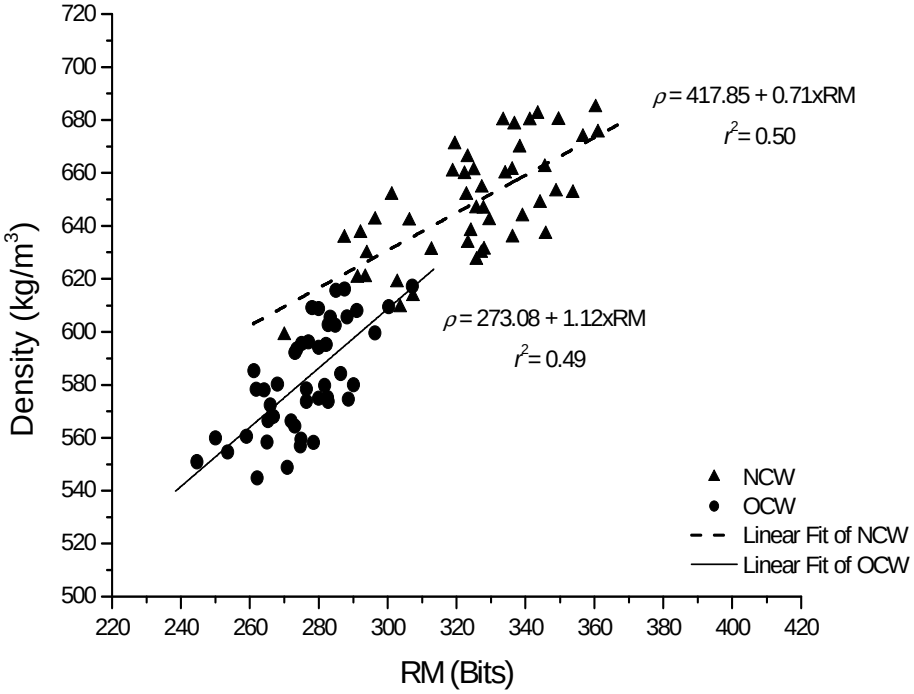

(a)

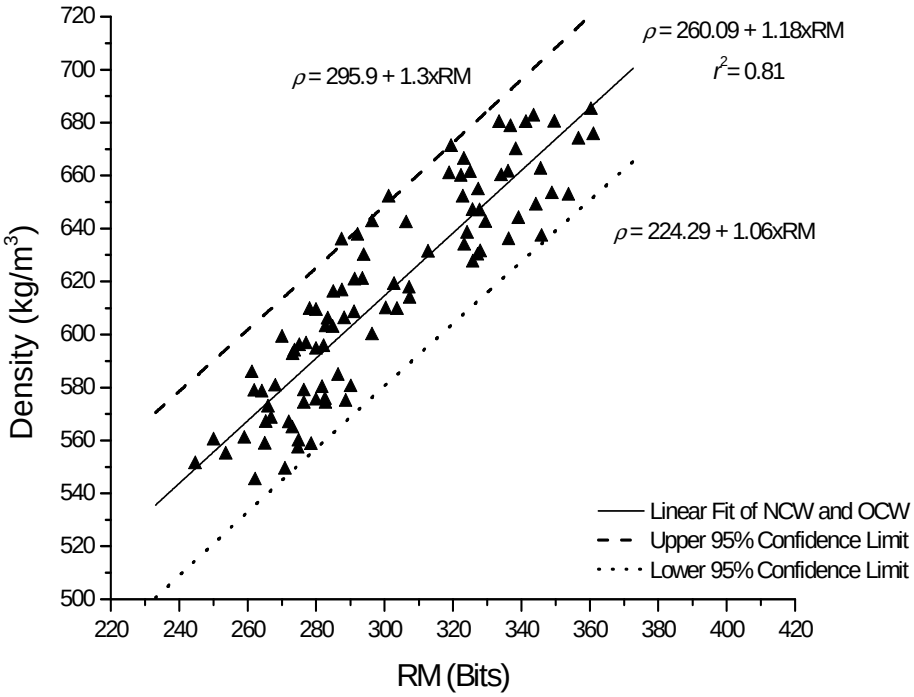

(b)

Figure 6 – Relation between *RM* and density: (a) partial results and (b) global results.

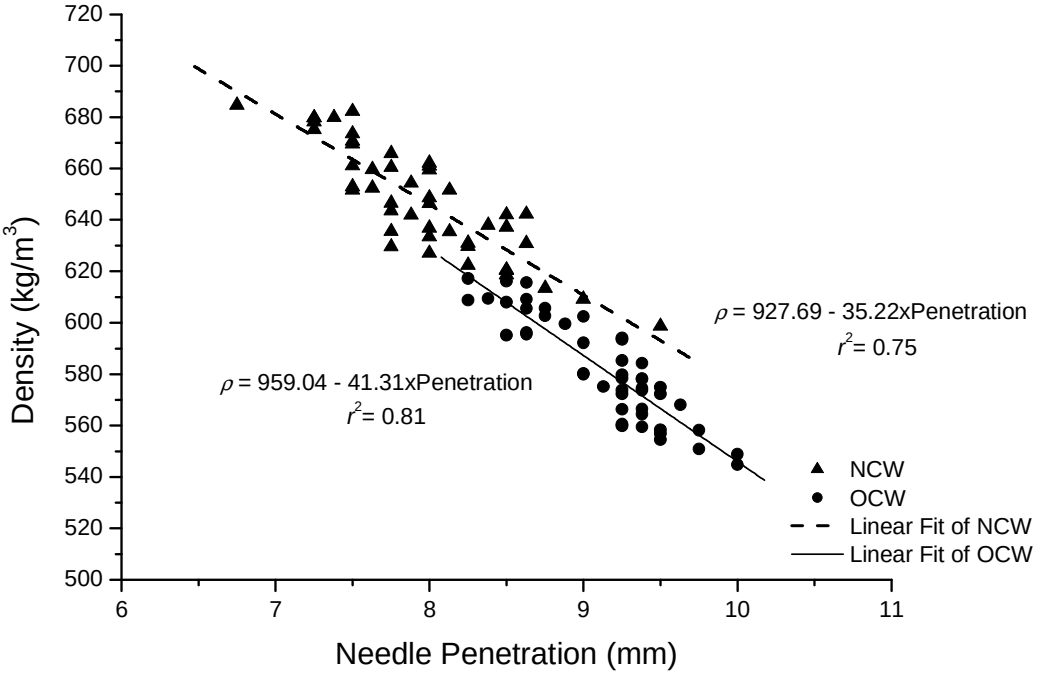

(a)

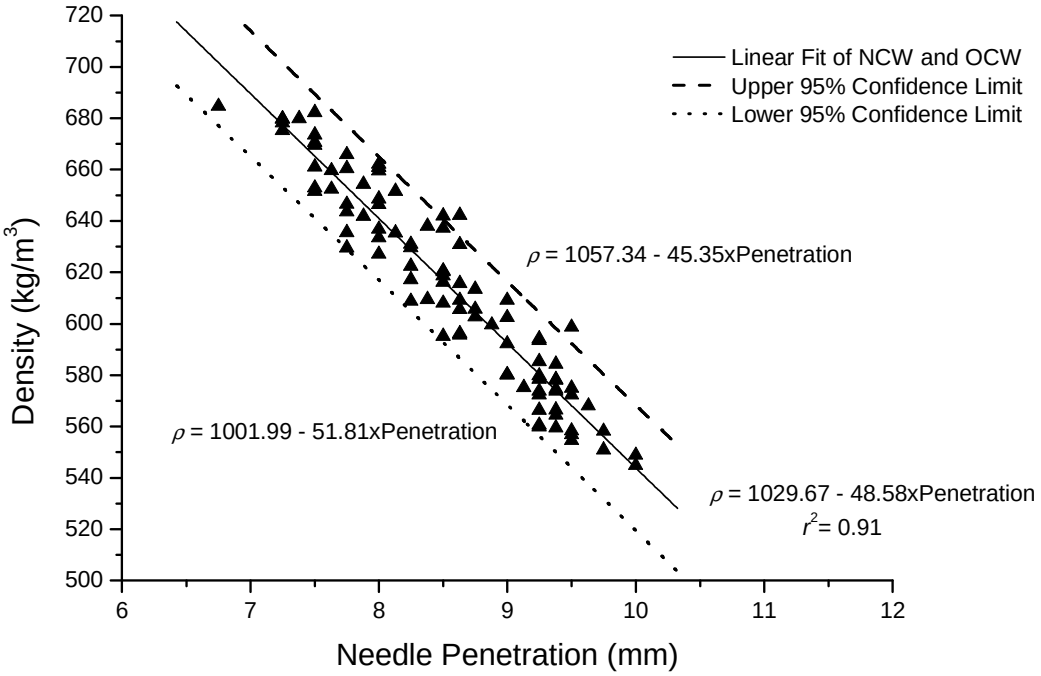

(b)

Figure 7 – Relation between needle penetration (Pilodyn) and density: (a) partial results and (b) global results.

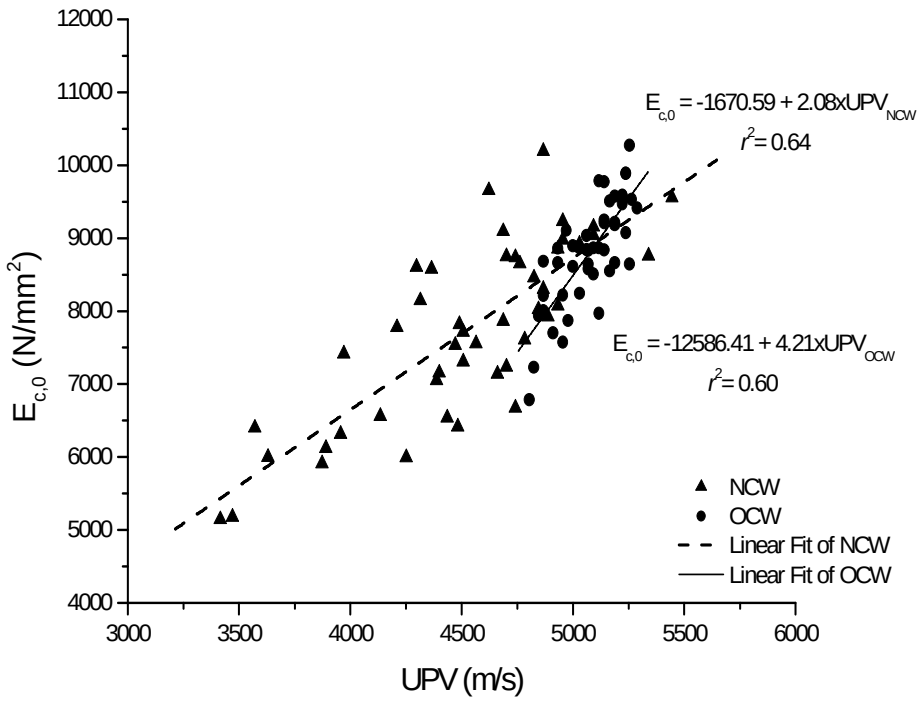

Figure 8 – Relation between UPV the and $E_{c,0}$, using the Indirect Method. Both NCW and OCW are considered.

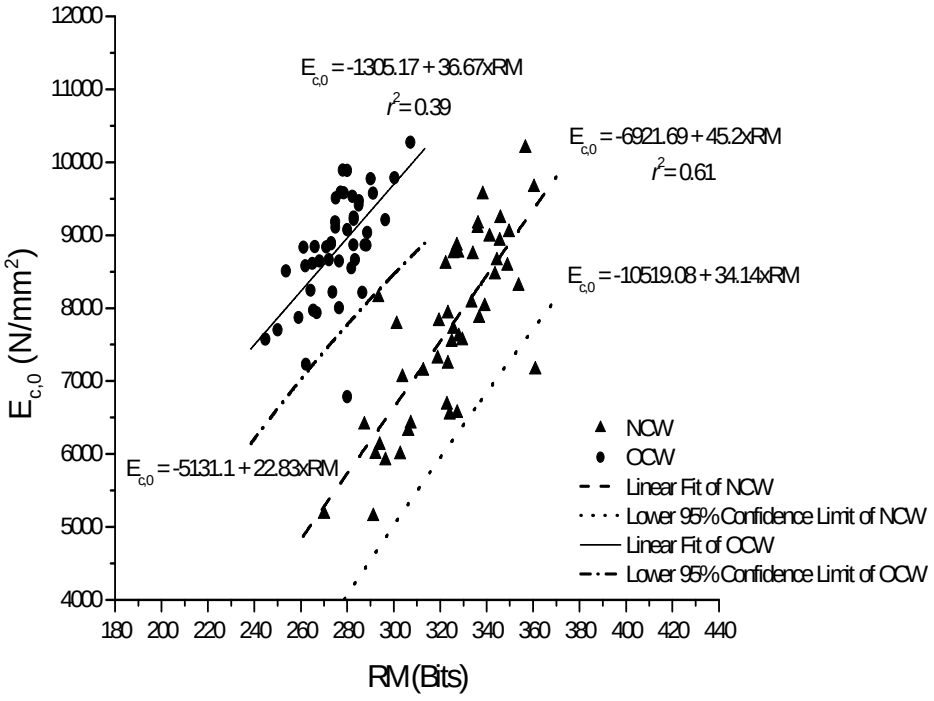

Figure 9 – Relation between RM and $E_{c,0}$. Both NCW and OCW are considered.

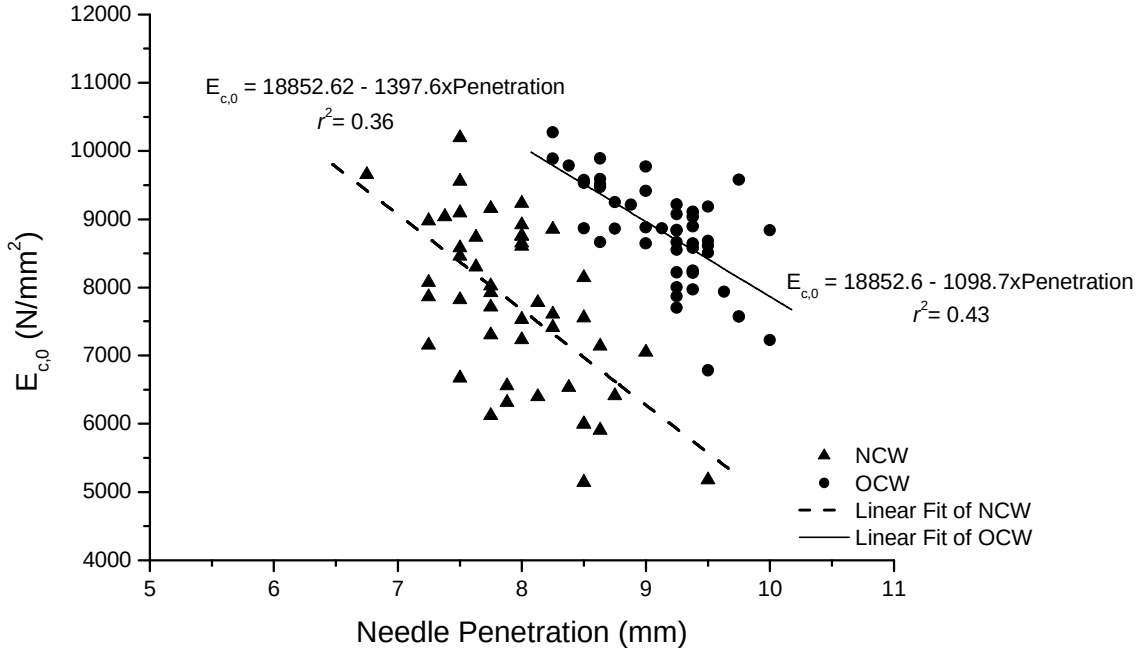

Figure 10 – Relation between needle penetration and $E_{c,0}$ for the NCW and OCW groups.

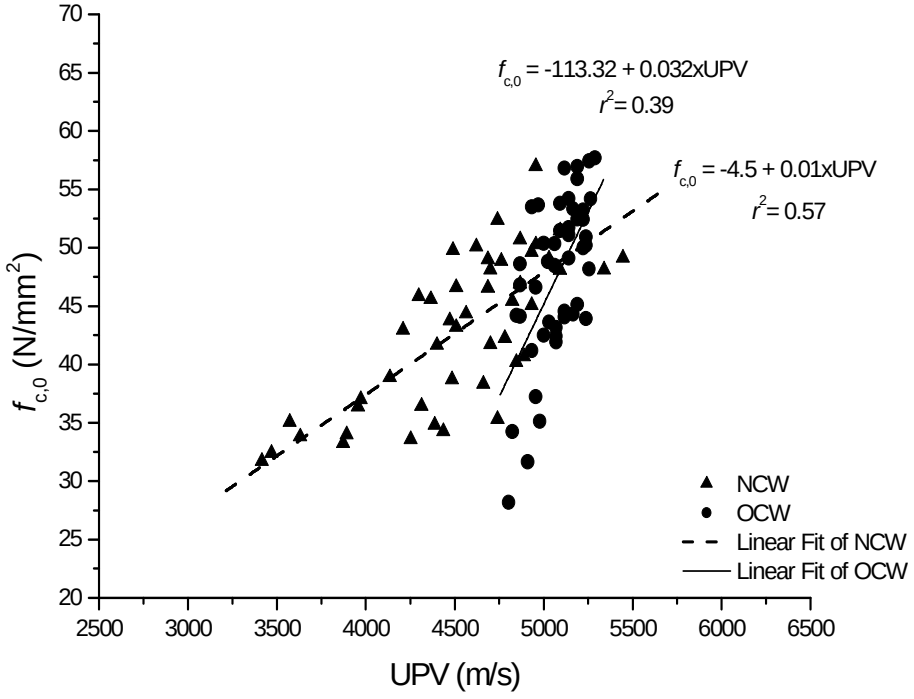

Figure 11 – Relation between the UPV and $f_{c,0}$, using the Indirect Method. Both NCW and OCW are considered.

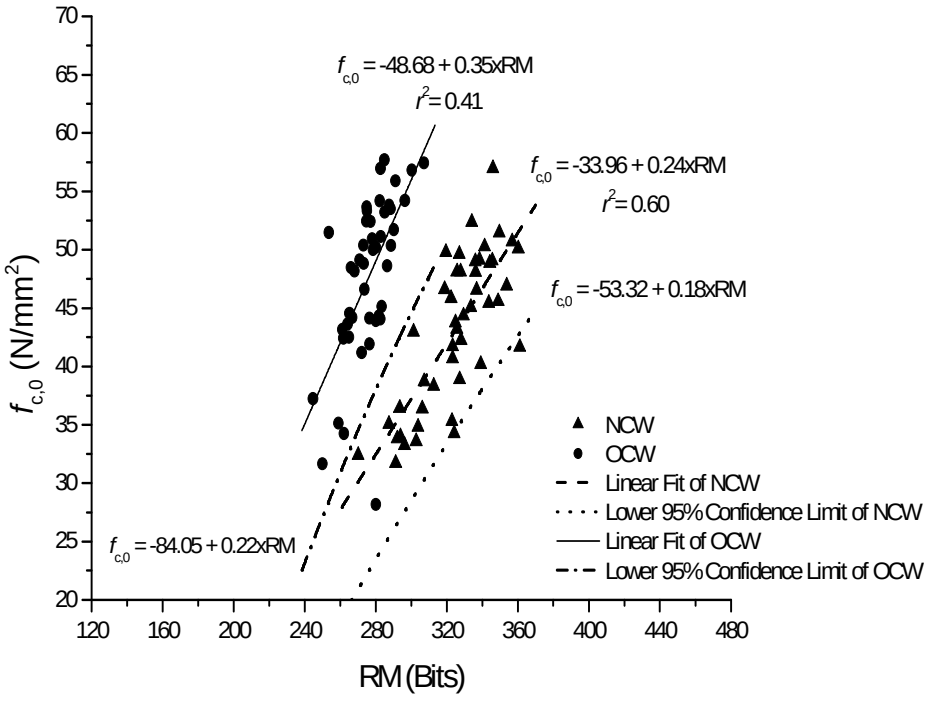

Figure 12 – Relation between RM and $f_{c,0}$ for the NCW and OCW groups.

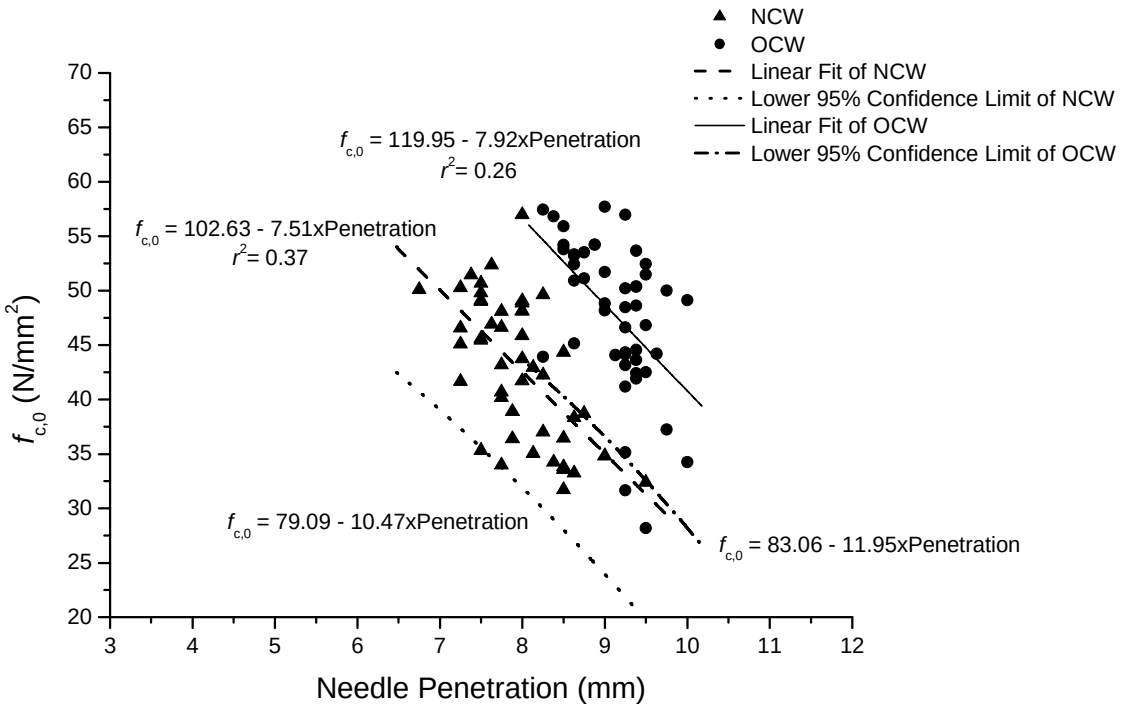

Figure 13 – Relation between needle penetration and $f_{c,0}$ for the NCW and OCW groups.

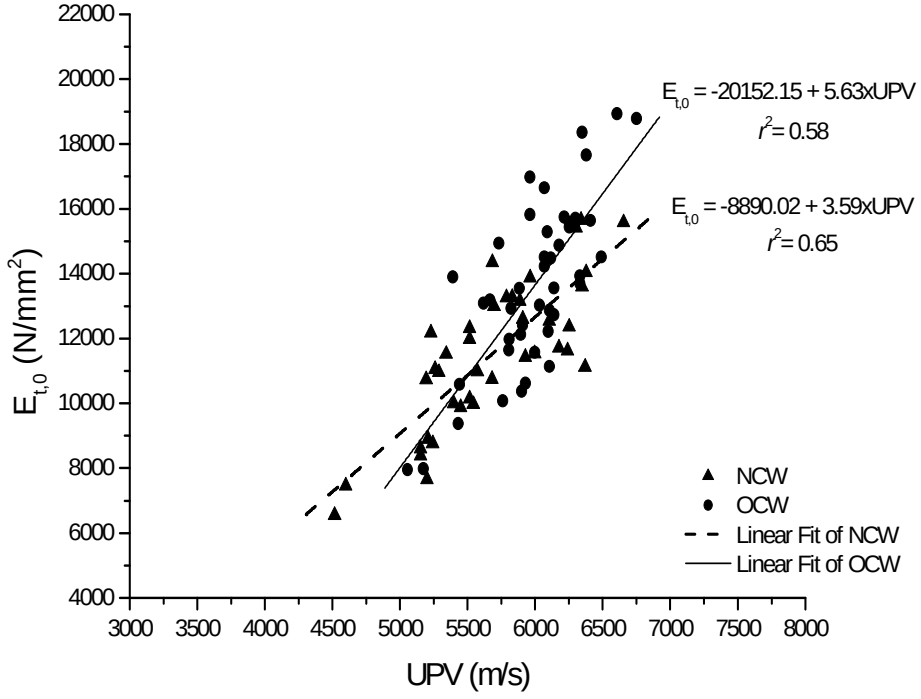

Figure 14 – Relation between the UPV and $E_{t,0}$ for the NCW and OCW groups.

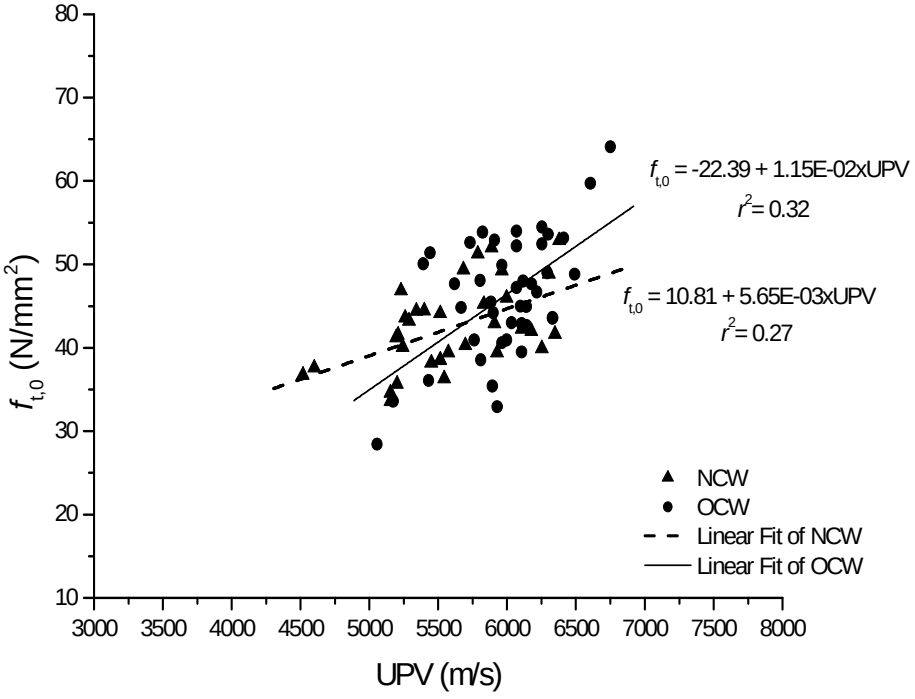

Figure 15 – Relation between the UPV and $f_{t,0}$ for the NCW and OCW groups.

Table 1 – Mean density and number of specimens considered in each group

	Compression Tests		**Tension Tests**	
	NCW	**OCW**	**NCW**	**OCW**
no. specimens	47	47	42	42
ρ_m (kg/m³)	647.8	581.8	604.3	597.5
CV (%)	3	3	10	10

Table 2 – Mechanical properties of chestnut wood in compression and tension parallel to the grain

	Compression (Total)		**Compression (NCW)**					**Compression (OCW)**				
no. specimens	94			47					47			
	$E_{c,0}$ (N/mm²)	$f_{c,0}$ (N/mm²)	$E_{c,0}$ (N/mm²)	ν_{LR} (-)	ν_{TR} (-)	ν_{LT} (-)	$f_{c,0}$ (N/mm²)	$E_{c,0}$ (N/mm²)	ν_{LR} (-)	ν_{TR} (-)	ν_{LT} (-)	$f_{c,0}$ (N/mm²)
Average	8.3E+03	45.3	7.7E+03	0.31	0.71	0.31	42.9	8.8E+03	0.31	0.72	0.28	47.6
CV(%)	12	14	16	14	13	30	15	8	14	13	27	14
	Tension (Total)		**Tension (NCW)**					**Tension (OCW)**				
No. specimens	84		42	---	---	15	42	42	---	---	15	42
	$E_{t,0}$ (N/mm²)	$f_{t,0}$ (N/mm²)	$E_{t,0}$ (N/mm²)	ν_{LR} (-)	ν_{TR} (-)	ν_{LT} (-)	$f_{t,0}$ (N/mm²)	$E_{t,0}$ (N/mm²)	ν_{LR} (-)	ν_{TR} (-)	ν_{LT} (-)	$f_{t,0}$ (N/mm²)
Average	12.6E+03	47.8	11.5E+03	---	---	0.45	47.4	13.7E+03	---	---	0.44	48.1
CV(%)	19	26	19	---	---	12	29	19	---	---	13	23

Table 3 – Influence of the age of wood in the UPV (Indirect Method). Note that the distance between transducers is different for the tension and compression tests

	UPV (m/s)		**UPV (m/s)**	
	Compression		**Tension**	
	NCW	**OCW**	**NCW**	**OCW**
Average	4526.8	5079.0	5678.0	6007.3
CV (%)	10	3	9	6
	Total			
Average	4802.9		5842.6	
CV (%)	9		8	

Table 4 – Comparison between the average values of mechanical parameters for compression and tension parallel to the grain

NCW		**OCW**	
$E_{t,0}/E_{c,0}$	$f_{t,0}/f_{c,0}$	$E_{t,0}/E_{c,0}$	$f_{t,0}/f_{c,0}$
1.49	1.11	1.56	1.01
Total			
$E_{t,0,total}/E_{c,0,total}$		$f_{t,0,total}/f_{c,0,total}$	
1.53		1.06	